14th World Congress in Computational Mechanics (WCCM)
ECCOMAS Congress 2020
Virtual Congress: 11 – 15 January 2021
F. Chinesta, R. Abgrall, O. Allix and M. Kaliske (Eds)

FORCE DISTRIBUTION ALONG TREE BRANCH – STATIC ANALYSIS

VOJÁČKOVÁ BARBORA[1], TIPPNER JAN[2] AND DLOUHÁ JANA[3]

[1]Faculty of Forestry and Wood Technology, Mendel University in Brno
Zemědělská 3, Brno 613 00, Czech Republic
barbora.vojackova@mendelu.

[2]Faculty of Forestry and Wood Technology, Mendel University in Brno
Zemědělská 3, Brno 613 00, Czech Republic
jan.tippner@mendelu.cz

[3] Université de Lorraine, AgroParisTech, INRAE, UMR Silva
5400 Nancy, France
jana.dlouha@.inrae.fr

Key words: Tree stability, Single-point loading, Multi-point loading, Finite element method, Tapered beams.

Abstract. The standard approach of tree stability assessment assumes that wind force is applied in a unique point (centre of gravity). Such a description of the loading brings a significant simplification of the reality, where the tree stem is submitted to multiple forces distributed from higher-order branches to lower order one. The aim of this study is to describe the influence of the simplification by comparison of branch response (deflection curve, bending moment) in the case of single- and the multi-point loading.

Four beam-like models were built in ANSYS APDL according to geometry (tapered beams with realistic elliptical cross-sections) and material properties (shear included) of real tested branches. The models were experimentally validated in the case of single-point loading and consequently used for simulations of various loading scenarios. The distribution of force along the branches, by weighted division of total wind force according to different properties of branches, was applied. The branch response differs between single- and multi-point loading in the case of deflection curve, whereas the bending moment at branch anchorage is comparable.

1 INTRODUCTION

Trees are exposed to different kinds of mechanical loading as wind, snow and ice [1,2,3], where the wind is considered to be the major one [4]. The evaluation of tree response to wind load is a key aspect of tree stability assessment. In general the assessment is based on analytical calculations of tree or branch bearing capacity to expected loading induced by wind [5,6]. Result of this calculation can be significantly changed by the variability in wind load description. Therefore high effort is dedicated to precise description of force magnitude,

which is defined by the profile of wind velocity, frontal area and drag coefficient [7]. These parameters are deeply investigated in relation to factors, which can influence them, as for example terrain characteristics [8] or crown reconfiguration [9,10]. Despite the effort for precise calculation of force magnitude, its application as a continuous load corresponding to reality is limited. In practice the force is assumed to be applied in the centre of gravity and resulting bending moment at observed position is computed [11]. Also the device supported methods as tree pulling test apply the load to the single-point [12]. Even there is no option to use the centre of gravity position [13] and the level of loading is usually lower. Similar approach is used in experimental method of "pull and release" test where dynamic tree response is observed [14]. During last decades, the numerical solutions are used to get closer to real load considering complex multi-point loading and response [15,16,17]. However, certain level of simplification is still required. The aim of this study on small but structural branches is to provide an overview about the effect of load distribution to the deflection curve and bending moments. Deflection curve provides overall information about the branch response including shape and material properties [7,18], while bending moment is defined only by the force magnitude and its position. The estimation and application of bending moments as possibility for numerical setup was recommended [19]. Therefore the character of bending moments along the main axis and individual components at branch anchorage are observed in the following study as well.

2 METHODOLOGY

2.1 Measurement

Four branches of two species were pruned from top part of solitary urban trees; two branches from birch (*Betula pendula* R.) and two from horse chestnut (*Aesculus hippocastanum* L.) e. These branches were anchorage to the holder (metal tube) in the same position (angle) as they have been growing at the tree (Tab. 1). White tape markers were placed 15 cm from each other along the main axis of branches.

Branches were pulled in vertical and horizontal direction by force applied in the centre of gravity (Fig. 1). The force was measured by weighing scale (Kern HDB, precision 5g). The magnitude of vertical force representing added mass (F_v) and horizontal force representing wind (F_h) was similar for both directions (Tab. 1). The motion of the branches during loading was recorded by camera Canon EOS700D (precision 1.6 mm, 0.2 fps) placed perpendicularly to pulling direction. The displacement of main axis at the position of markers was processed in Mercury (Digital Image Correlation software, Sobriety ltd.).

The dimensions measured on all branches were: diameters at the marker position (on 15 cm sections) along the main axis in vertical and horizontal directions (d_v,d_h), length of the main axis (l_a), centre of gravity position (l_g), overall mass (m) and angle of anchorage (α). Consequently the side branches were cut off close to their leaf area. Individual parts were weighted to obtain mass ($m_{s1,2..i}$), captured by camera to do image analysis in RealTree (Sobritey, ltd.) to obtain frontal area ($a_{s1,2..i}$) of each side branch (branches of higher order). At the same time for each side branch the angle orientation along the circumference of main axis was measured ($p_{1..i}$), together with base diameter (d_{si}), angle of anchorage ($\alpha_{s1..i}$), distance of side branch base from marker ($l_{t1..i}$) and overall length of uncut parts ($l_{s1..i}$).

The dynamic longitudinal (E_L) and shear moduli (G) of elasticity were repeatedly measured for each branch on the 30 cm long sections by BING® method (Cirad FR) (Tab. 1). From the same section the green wood density was obtained (weight of green wood divided by section volume).

Table 1: Main parameters of measured branches used in FEM: α – angle of branch anchorage (same as possition in crown, l_g centre of gravity possition, l_a length of main axis, d_{v1}/d_{h1} diameter at branch base in verical/horizontal direction, m overall mass, F_v force applied in vertical direction (added mass representation), F_h force applied in horizontal direction (wind representation), E_L/SD dynamic longitudinal elastic modulus/standard deviation, G/SD shear modulus/stadard deviation.

	α (°)	l_g (m)	l_a (m)	d_{v1} (cm)	d_{h1} (cm)	m (kg)	F_a (N)	F_s (N)	E_L/SD (Mpa)	G/SD (Mpa)
No. 1 Birch	46	1.56	2.90	36.63	37.58	3.95	19	20	4819/46	800/123
No. 2 Birch	62	1.71	3.62	40.39	41.08	5.20	47	49	8008/27	574/3
No. 3 Chestnut	49	1.35	2.68	35.19	36.95	2.65	34	34	4985/569	516/47
No. 4 Chestnut	65	1.43	2.73	43.01	40.49	3.23	48	48	4658/812	688/298

2.2 Numerical simulation

Static structural analyses for linear-elastic behaviour with assumption of large deformation were performed in Mechanical APDL (Ansys® Academic Research Mechanical, Release 2020 R2, ANSYS, Inc.). The geometry of finite element model (FEM) representing branches were defined according to measured dimensions and simplified to beam construction with a straight main axis (Fig. 1). Cross-sections of beam elements (BEAM 189, Help System, Mechanical APDL, Element reference, ANSYS, Inc.) were defined in 15 cm long sections (markers position) by user defined option (ASEC command) for the main axis. Input values of cross-sections (moments of inertia, section areas) were calculated for elliptical shape from d_v and d_h. Cross-sections of side branches were defined as circular and dimensioned by $d_{si.}$ The bark thickness (2mm for main axis, 1 mm for side branches) was subtracted from the diameters. The key-points were defined at the beginning and the end of each section of the main axis and on the end and top of each side branch. The key points between main axis and base of side branches were bounded by constrain equations (CE command) with full transfer of boundary conditions.

Shear modulus was defined in material model to take into account anisotropic character of wood. Values (Tab. 1) were set according the average values from experiment for each branch. Same values along the main axis and for side branches were used for the first set of analyses.

In the first load step the FEM branches were loaded by gravity (ACEL command, 9.81 m/s), added mass of side branches on their tops and fully anchorage at the same position as during the experiment. The state after first load step represents branch position before loading by single- or multi- point force, where real branches are naturally loaded by self-weight. To obtain this state in the geometry of FEM branches is built in the unloaded state and it is subsequently loaded by gravity. For the second load step small initial displacement (ux,uy,uz) and rotation (rotx, roty) were defined at the position of anchorage according the

initial movement of the holder. Six loading scenarios were performed by FEM. First two applied single-point loading in the centre of gravity according to experiment 1) in horizontal direction and 2) in vertical direction. These were followed by a set of loadings in horizontal direction with different force distribution. Force applied at the top (end point) of each side branch represented a part of the total force weighted by 1a) side branch diameter (EP diameter), 1b) side branch mass (EP mass) and 1c) side branch leaf area (EP area). As the last option 1d) the force was distributed to all key points within the FEM, where as distribution factor the frontal area of each branch and leaf section was chosen (KP area). Frontal area was chosen for the first set of analyses as factor which is directly interacting with wind (eq. 1), therefore it is naturally used for the force definition within other studies [16]. Force distribution according to mass was chosen as additional parameter which is representative for the description of load, while diameter represents dimension which can be precisely measured and is in relation to mass and leaf area according alometric equations [20,21]. The correlations within measured values of mass, area and diameters were verified by Spearman correlation coefficients (0.68-0.89).

As output parameters the displacements, bending moment components at the position of anchorage and resultant of bending moments along the branch were chosen. The displacements were listed for nodes corresponding to ones observed in experiment (markers position). For the validation the position of points after first load step (load by gravity), displacements for loading in vertical direction (added mass) and horizontal direction (side pulling) were plotted and character of the deflection curve was observed. The fifth marker was selected as representative for validation because this position includes the behaviour of the entire lower part, but is not affected by irregularities of real branches and measurements errors. These were caused by the movement of leaves in higher positions. For following analyses of loading scenarios the displacements (deflection curve) and bending moments were compared. The coordinate system of bending moment components with relation to branch position and loading is presented in Fig. 1.

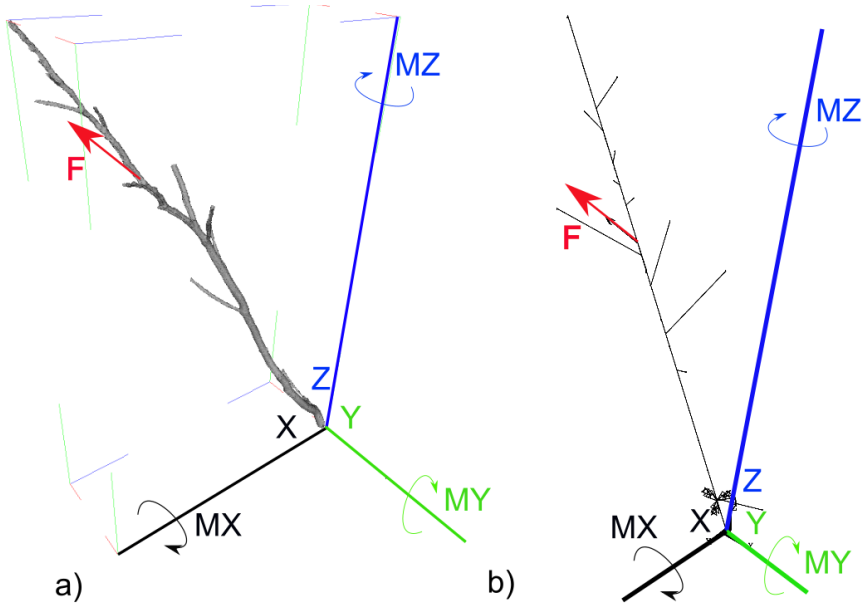

Figure 1: Illustration of branch no. 4 in relation to observed components of bending moment (*MX, MY, MZ*) and schematic representation of single-point force position (*F*) in the centre of gravity: a) real branch geometry, b) simplified beam structure FEM branch.

3 RESULTS AND DISCUSSION

3.1 Experiment and FEM Validation

Measured positions and displacements of branches were used for validation of FEM. The position of markers along main axis between FEM and experimental branches corresponds in lower parts (up to 60cm of the branch length), except the branch no. 4 (Fig. 2a). The main axis of branch no. 4 was curved closely to the anchorage point and therefore the difference between FEM and original position is visible here. For branches no. 2 and 3 there is visible deviation, caused by curvature of main axis in the upper part of the branches. Simplified geometry of FEM which didn't considered curvature of main axis probably influences the response of branch loaded by added weight (vertical loading) (Fig. 2c). Even the relative error (RE) is up to 22.9% at the position of marker five there is visible different character of FEM deflection curve for branch no 4. Also the deviation of branches no. 2 and 3 occurred in upper parts what follows the effect of geometry, whereas the RE at marker 5 is lower than in case of branch no. 4 (15.4%, -5.5%), as the behaviour of lower part is corresponding more to the measurement. The character of branch no. 1 FEM deflection curve fits measurement well, correspondingly to the fit of original position, although locally the RE is 17.8%. In the case of horizontal loading (Fig. 1b) character of FEM deflection curve corresponds to measurement in all cases, regardless the deviation in original position. The horizontal load was crucial for experimental validations of FEM because it represents loading by the wind.

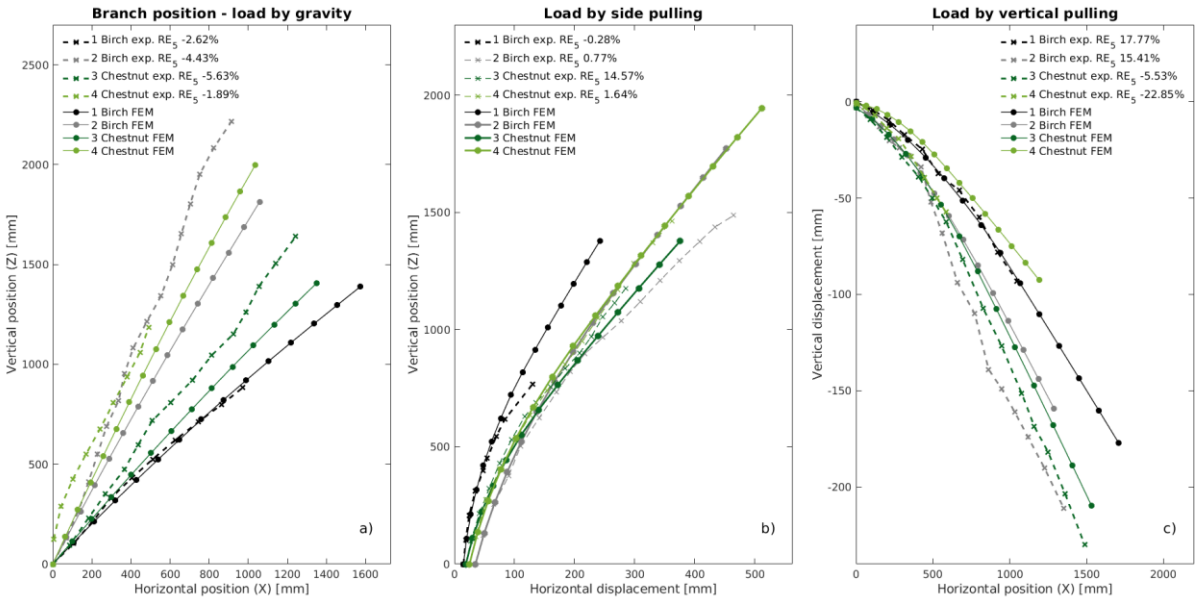

Figure 2: Comparison of FEM and measured displacement along branches: a) original branch position compared with FEM branch loaded by gravity (ACEL), b) branches loaded by side one-point pulling (horizontal load) c) branches loaded by added weight in centre of gravity (vertical load). RE is relative error between FEM and experiment at the position of fifth marker.

Considering the high variation in material properties (Tab. 1) the FEM approximates branch response in sufficient way (curve course and RE in displacements Fig. 2). The prediction of FEM could be further improved by more realistic definition of material properties with respect of its distribution along branch in upper parts, since the variable MOE in branches was proved [22]. For this study the material properties remains homogenous along branches to eliminate variability. At the other side, the initial rotation at the branch anchorage significantly influenced the validation and couldn't be omitted as reported previously [23].

3.2 Single- and Multi-point analysis - deflection

Differences in in displacements among loading scenarios (Fig. 3) reveal the higher deflection of the main axis in the upper part of the branch in all cases for distributed loading compared to the single point horizontal loading. This phenomen is more obvious for the Chestnut branches (branch no. 3, 4; Fig. 3 c, d).

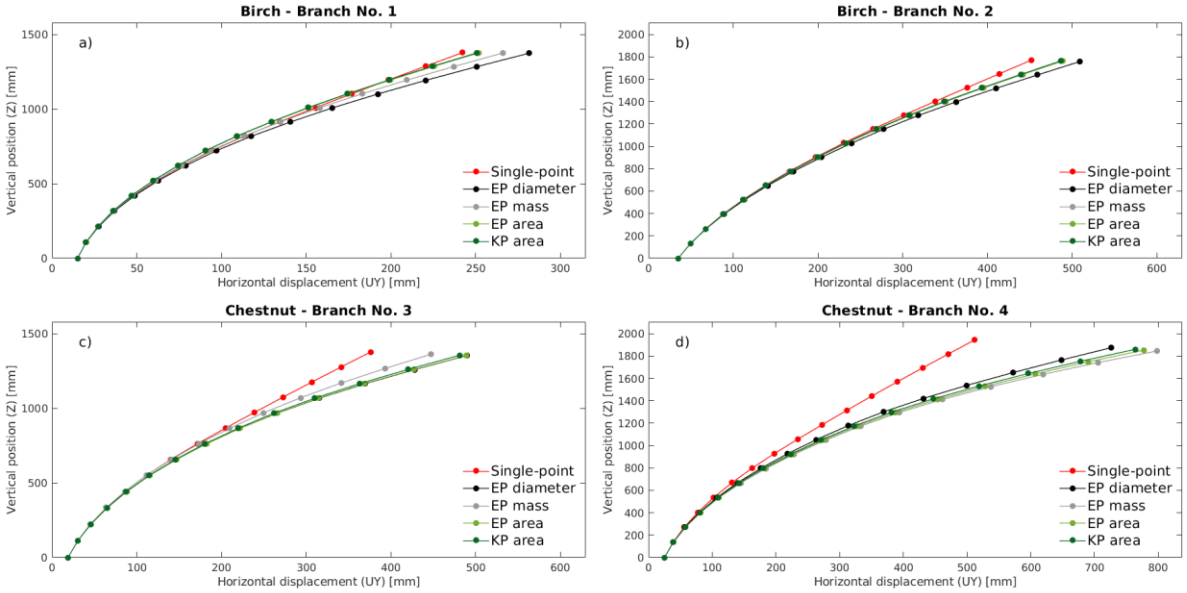

Figure 3: Horizontal displacements of FEM branches during different variants of horizontal loading. EP – loading on end points of side branches distributed according diameter, mass and area; KP – loading on all key points within FEM.

Relative errors of horizontal displacements along branches between single- and different kinds of multi-point loading reveal the higher deflection of upper parts for multi-point variants for birches (tree no. 1, 2, Fig. 4 a, b), this is not so visible in Fig. 3 (comparison based on absolute values). This shows that the curvature (nonlinearity) of birch branches displacements is higher in comparison to the single-point scenario, while chestnut branches deviates more along the whole branch. Especially branch no. 4 begins to deviate in lower parts so the whole branch exhibit higher inclination during the multipoint loading. Also the maximum RE on position of the marker 14 (1.95 m from anchorage) is in the case of branch no. 4 highest (43.9%), followed by second chestnut (branch no. 3) 30.2%. For birches the maximum RE at the same position is 10.9% for branch no. 2 and 13.7% for branch no. 1. The higher curvature of branches in the case of multi-point loading follows the pattern of bending moments along the main axis (3.4).

The scenarios of weighted force distribution according area is closely related to each other regardless of distribution on the end points of side branches (EP area) or on the all key-points within FEM (KP area), as the frontal area of branches is probably insignificant in relation to leaf area (2-7%). Except branch no. 3, where overall mass was lowest (Tab. 1), the force distribution according mass and area are closer than diameter distribution. This corresponds to higher correlation of mass and leaf area (sp. coeff. 0.89) than in the case of diameter (0.78 mass/diameter and 0.68 area/diameter). The differences among various multi-point load distributions are lower for chestnut trees (up to 10.9%, at marker 14) than between multi- and single point loading. While for birch branches difference among multi-point distribution (up to 11.8%, at marker no. 14) is similar to variation with single-point loading. However, in general, the branch deflection curve differs between single- and multi-point scenarios, but the difference between multi-point loading scenarios is not significant (approx. up to 12%).

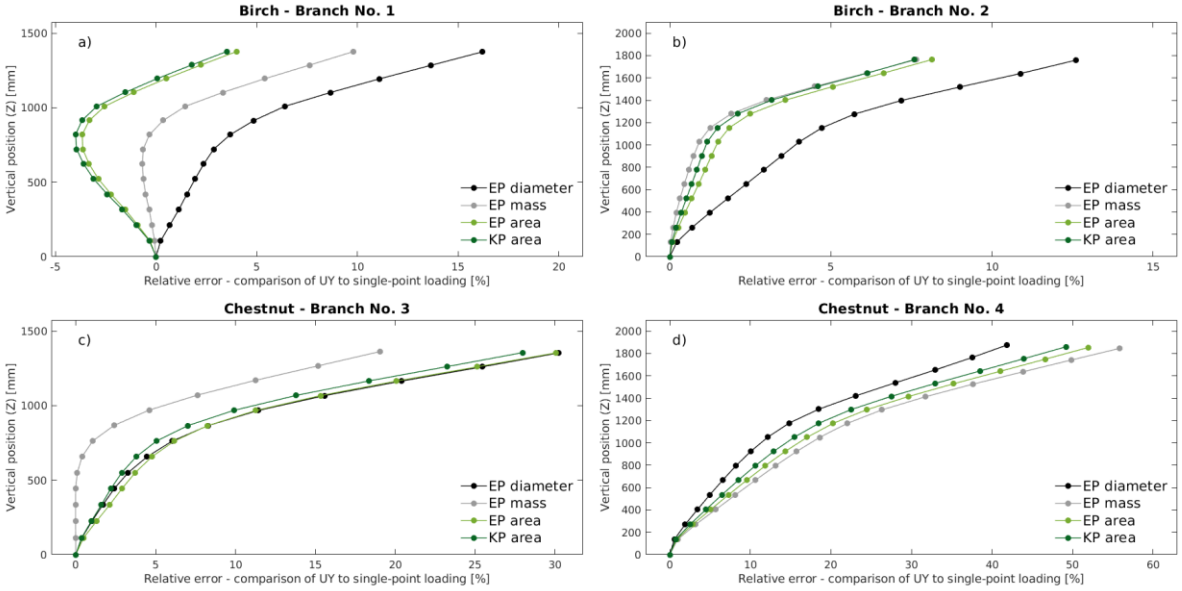

Figure 4: Relative errors in horizontal displacement of FEM branches between single-point and other kind of loading: EP loading on end points of side branches, KP loading on all key points within FEM.

3.3 Single- and Multi-point analysis – bending moment

Fig. 5 illustrates differences in bending moments (MX, MY, MZ) at the anchorage point between single- and multi-point loading. In general values for the single-point are lower than for multi-point loading. However bending moments for loading variants are comparable (differences up to 9.4%) for branches no. 1, 2, 3. Higher differences (up to 27.6%) between loading variants in the case of branch no. 4. corresponds to the lowest MY/MX ratio caused by highest portion of applied load in comparison to self-weighting.

For the most of branches the MX is the highest (ca. 30-80 Nm), where for example the single-point variant give MY at about 22-42% of MX for branch no. 2, 3, 4. The exceptional case of branch no. 1 when MY is higher than MX (126%) corresponds to the lowest ratio of applied force to self-weighting (0.5 in comparison to approx. 1.0, 1.3, 1.5 for branches no. 2, 3, 4). The situation is given by the angle of branch anchorage and horizontal distance between centre of gravity and anchorage point, when the lowest angle (inclination to the ground level – 46°) reveal moments in multiple directions. Whereas branches no. 2 and 4. with higher anchorage angle (62°, 65° - closer to vertical direction) induces lower MZ (up to 50%) in comparison to MX (lower MZ/MX ratio).

This variation within multi-point loading scenario corresponds to deviation in maximal displacement (3.2). MX has highest difference in comparison to single-point loading in the case of weighted force according the branch diameter for branches no. 1, 2, 3 (up to 7.7%). For branch no. 4 the highest difference is for scenario of weighted force according mass (up to 22.9%). The differences within the multi-point loading scenarios are smaller (up to 13.5%) than between multi- and single-point loadings, although the difference is there only up to 22.9% in MX and 27.6% in MY in bending moment components at the anchorage point. The difference increases with increasing applied loading vs. overall mass ratio.

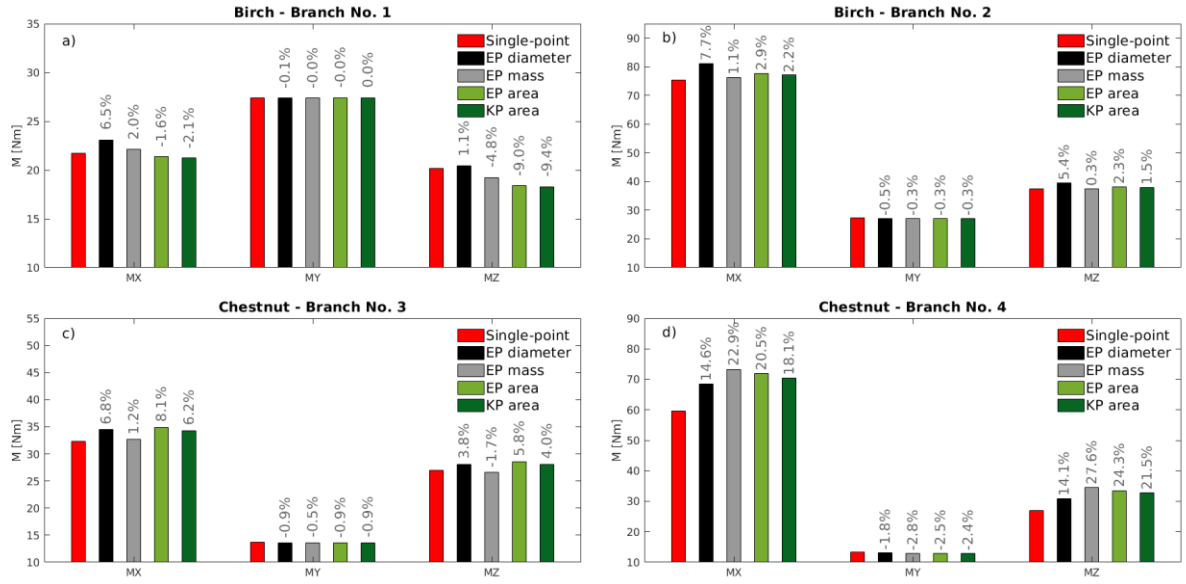

Figure 5: Bending moments for different kind of loading in three directions: MX – rotation around X axis, MY rotation around Y axis (direction of loading), MZ rotation around Z axis; EP loading on end points of side branches, KP loading on all key points within FEM.

3.4 Single- and Multi-point analysis – progress along the branch main axis

Bending moments (M_{sum}) along the main branch axis have similar character for single- and multi-point loading scenario. The most noticeable difference is at the position of applied force in single-point loading for branches no. 2, 3, 4 (Fig. 6). There is linear decrease of M_{sum} under position of loading (centre of gravity), followed by steep decrease of M_{sum} above it. The resulting M_{sum} above loading point in single-point case is induced by gravity. For multi-point variant the M_{sum} is more evenly distributed according applied force, although there is visible small change of curvature course (jump in derivation) also (Fig. 6 b, c, d – A). The distinctive change is not visible for branch no. 1, where the character of bending moments along the main axis is similar for all loading scenarios. This is caused by the low value of applied force in comparison to self-loading of branch (0.5 ratio) as mentioned in 3.3. The similar character of M_{sum} along the main axis for multi- and single-point scenarios shows that the load representation by force in the centre of gravity is sufficient even the level of simplification is high. The single-point vertical loading shows lower bending moment for branch no. 2 and 3 caused by higher anchorage angle (62°, 65° - closer to vertical direction). In contrary branch no. 1 shows higher bending moment induced by vertical loading as the combination of low anchorage angle and low rate of mass to applied side load influence the response. Higher M_{sum} in upper position corresponds to higher curvature for multi-point variants (3.3), but this effect is not correlated to area or mass of side branches. This phenomenon should be further verified by the higher number of measurement. The loading in the centre of gravity gave similar resulting bending moment at anchorage point; to assess the possibility of failure at the anchorage point under static loading the simplification of the single point loading is therefore convenient however this may change under dynamic loading.

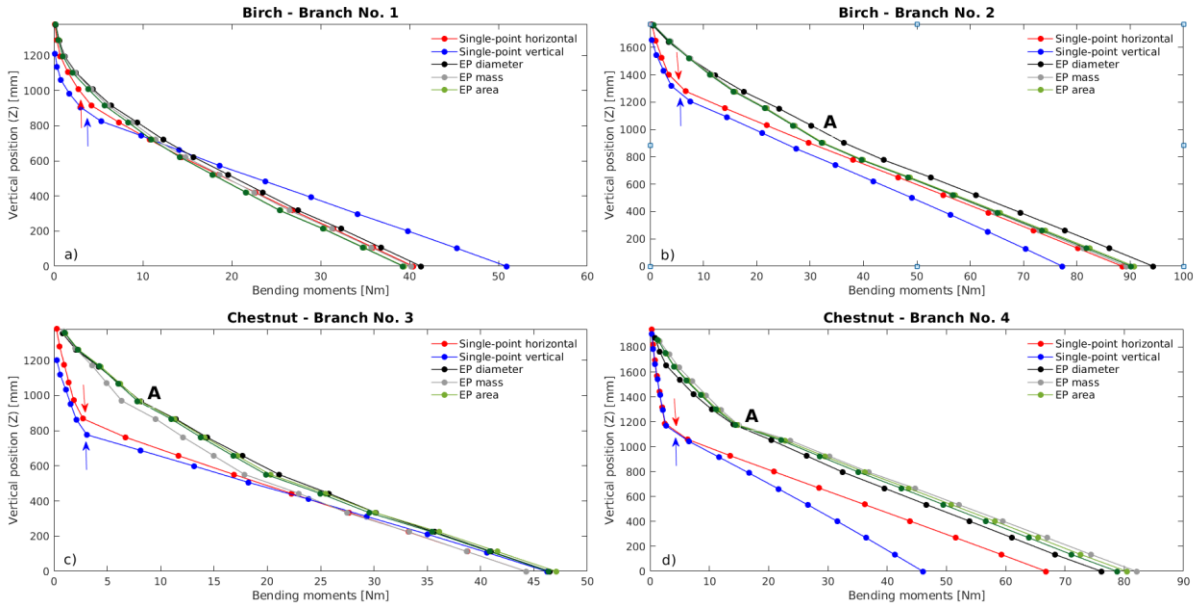

Figure 6: Progress of bending moment's vector along the branch for differenet kinds of loading. EP loading on end points of side branches, KP loading on all key points within FEM. Arrows plots point of single-point loading (centre of gravity).

11 CONCLUSIONS

Two birch and two chestnut structural branches (of diverse geometry) sampled in the higher crown of trees were used to study their displacement under horizontal and vertical loads. For these branches, the parametrical FEM were built and used for analyses of various loading scenarios. Despite the variability of selected branches the FEM was validated and provided results comparable with the experiment in all four cases. Consistency of results especially in case of the deflection curve shape and the case of bending moments along the branch axis confirms the FEM reliability. Such validated model can be used for further detailed analyses as for example assessment of gravity effect, the position of loading point or sensitivity analyses dedicated to the influence of geometry or material properties. Comparable results among loading scenarios confirm that the principle of branch loading by single-point force is applicable, as far as the force is applied in the centre of gravity. However, the influence of the ratio between the applied load vs. the overall mass should be investigated in more details. The bending moments appear to be valid for loading of lower order branches, for example crown sub-structuring with representing of branches by applying moment loading at branch anchorage point. The jump in the derivation of bending moments in both single- and also multi-point loading scenarios should be investigated in the following work.

12 ACKNOWLEDGEMENT

Research was funded under doctoral student's project of Barbora Vojáčková IGA no. 2018036. Experimental and numerical analysis of branch mechanical loading in cooperation of Mendel University in Brno, Faculty of Forestry and Wood Technology and Université de Lorraine, AgroParisTech, INRAE supported by grant of the French National Research

Agency (ANR) as part of the "Investissements d'Avenir" program (ANR-11-LABX-0002-01, Lab of Excellence ARBRE) and grant of Ministry of Education Youth and Sports in the Czech Republic (Tree Dynamics: Understanding of Mechanical Response to Loading, no. LL1909, ERC CZ).

REFERENCES

[1] Hale, S. E., Gardiner, B. A., Wellpott A., Bruce C. N. and Achim A. Wind Loading of Trees: Influence of Tree Size and Competition. *European Journal of Forest Research* (2012) **131**(1):203-17.

[2] Gregow, H., Peltola, H., Laapas, M., Seppo S. Combined Occurrence of Wind, Snow Loading and Soil Frost with Implications for Risks to Forestry in Finland under the Current and Changing Climatic Conditions. *Silva Fennica* (2011) **45**(1) (October 2010):35-54.

[3] Gaffrey, D. and Kniemeyer, O. The Elasto-Mechanical Behaviour of Douglas Fir, Its Sensitivity to Tree-Specific Properties, Wind and Snow Loads, and Implications for Stability - Simulation Study. *Journal of Forest Science* (2011) **48**(2):49-69.

[4] Gardiner, B., Berry, P., Moulia, B. Review: Wind impacts on plant growth, mechanics and damage. *Plant Science* (2016) **245**:94-118.

[5] Dahle, G.A., James, K.R., Kane, B., Grabosky, J.C. and Detter, A. A Review of Factors That Affect the Static Load-Bearing Capacity of Urban Trees. *Arboriculture and Urban Forestry* (2017) **43**(3):89-106.

[6] Peltola, H. M. Mechanical Stability of Trees under Static Loads. *American Journal of Botany* (2006) **93**(10):1501–11.

[7] Niklas, K. J., Spatz, H. CH. *Plant physics*. Chicago: University of Chicago Press (2012).

[8] Pirner, M. and Fischer, O. Zatížení staveb větrem. Praha: Informační centrum ČKAIT Vol. I. (2003).

[9] Brüchert, F., Gardiner, B. The Effect of Wind Exposure on the Tree Aerial Architecture and Biomechanics of Sitka Spruce (*Picea Sitchensis*, Pinaceae). *American Journal of Botany* (2006) **93**(10):1512-21.

[10] Rudnicki, M., Mitchell, S. J. and Novak, M. D. Wind Tunnel Measurements of Crown Streamlining and Drag Relationships for Three Conifer Species. *Canadian Journal of Forest Research* (2004) **34**(3):666-76.

[11] Niklas, K. J. and Spatz, H. Methods for calculating factors of safety for plant stems. *The Journal of Experimental Biology* (1999) **202**: 3273-3280.

[12] van Wassenaer P. and Richardson, M. A Review of Tree Risk Assessment Using Minimally Invasive Technologies and Two Case Studies. *Arboricultural Journal* (2009). **32**:275-292.

[13] Moore, J. R. Differences in maximum resistive bending moments of Pinus radiate trees grown on a range of soil types. *Forest Ecology and Management* (2020). **135**:63-71.

[14] James, K. R., Nicholas H. and Ades, P. K. Mechanical Stability of Trees under Dynamic Loads. *American Journal of Botany* (2006) 93(10):1522–30.

[15] Yang, M., Défossez, P. and Dupont, S. et al. *A root-to-foliage tree dynamic model for gusty winds during windstorm*. Agricultural and Forest Meteorology (2020). **287**:107949.

[16] Jackson, T., Shenkin, A., Wellpott, A., Calders, K., Origo, N., Disney, M., Burt, A., Raumonen, P., Gardiner, B., Herold, M., Fourcaud, T. and Malhia, Y. Finite element analysis of trees in the wind based on terrestrial laser scanning data. *Agricultural and Forest Meteorology* (2019). **265**:137-144.

[17] Ciftci, C., Sergio F. B., Kane, B. and Arwade, S. R. The Effect of Crown Architecture on Dynamic Amplification Factor of an Open-Grown Sugar Maple (*Acer Saccharum* L.). *Trees - Structure and Function* (2013) **27**(4): 1175-89.

[18] Neild, S. A. and Wood, C. J. Estimating Stem and Root-Anchorage Flexibility in Trees. *Tree Physiology* (1999) **19**:141-51.

[19] Dellwik, E., van der Laan, M. P., Angelou, N., Mann, J. and Sogachev, A. Observed and modeled near-wake flow behind a solitary tree. *Agricultural and Forest Meteorology* (2019) **265**:78-87.

[20] Dahle, G. A. and Grabosky, J. C. Allometric patterns in *Acer platanoides* (Aceraceae) branches. *Trees (*2010) 24:321-326.

[21] Yoon K. T, Park, Ch., Lee, S. J., Ko, S., Kim, K. N, Son, Y., Lee, K. H., Oh, S., Lee, W. and Son Y. et al. Allometric equations for estimating the aboveground volume of five common urban street tree species in Daegu, Korea. *Urban Forestry & Urban Greening* (2013) 12: 344-349.

[22] Dahle, G. A. and Grabosky J. C. Variation in modulus of elasticity (*E*) along *Acer platanoides* L. (Aceraceae) branches. *Urban Forestry & Urban Greening* (2010) 9: 227-233.

[23] Vojáčková, B., Tippner, J., Horáček, P., Praus, L., Sebera, V. and Brabec, M. Numerical Analysis of Branch Mechanical Response to Loading. *Arboriculture & Urban Forestry* (2019). **45**(4): 120-131.